SPIN OBSERVABLES IN FEW-BODY SYSTEMS: RESULTS AND PROSPECTS FROM JEFFERSON LAB

C.W. de Jager
Jefferson Laboratory, 12000 Jefferson Avenue,
Newport News, VA 23606, USA

Selected highlights are presented of that part of the research program at Jefferson Lab, which is focused on properties of nucleons and of few-body systems. The majority of the experiments described use a polarized beam in conjunction with a polarized target or an ejectile polarimeter. All depend heavily on the high quality of the beam produced by the CEBAF facility.

1 Introduction

Spin-dependent electron scattering offers the potential to enhance our understanding of nucleon and nuclear structure through its access to interference terms between large and small components in the reaction amplitude. Electron-scattering experiments off polarized targets are now being carried out at a number of intermediate- and high-energy facilities. Spin observables from polarized deuterium are providing important information on the elusive neutron electric form factor G_E^n, the neutron spin structure function and the D-state component in the deuteron ground-state wave function. Polarized ^3He provides an alternative access to measure G_E^n or the neutron spin structure function. The first results obtained at the JLab facility clearly prove the impressive potential and range of a research program with a polarized electron beam and polarized targets.

2 The CEBAF Facility

CEBAF (Continuous Electron Beam Accelerator Facility) (see fig. 1) was designed to accelerate electrons to 4 GeV by recirculating the beam four times through two superconducting linacs, each producing an energy gain of 400 MeV per pass. Beam can be injected into the accelerator from either a thermionic or a polarized gun. In the polarized gun a GaAs cathode (bulk or strained) is illuminated by a 1497 MHz gain-switched diode laser, operated at 780, resp. 850 nm. A so-called hydrogen-cleaning technique (using an RF discharge in low-pressure hydrogen) has been extremely successful in cleaning the GaAs wafers and thus yielding very high quantum efficiencies. The polarization is measured at the injector with a 5 MeV Mott polarimeter and the polarization vector can be oriented with a Wien filter. Three independent slits at the

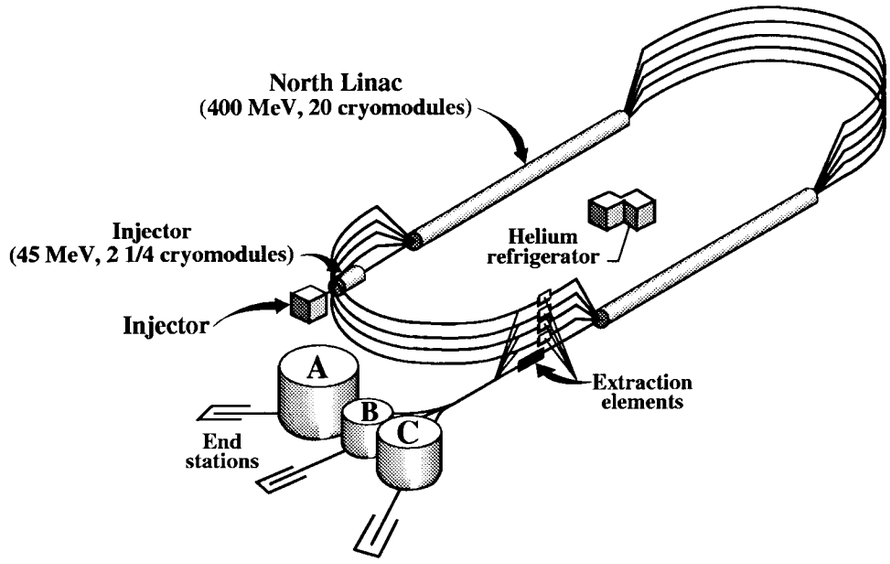

Figure 1: Lay-out of the CEBAF facility.

chopper are used to individually control the current to the three experimental Halls A, B and C.

Each linac contains 20 cryomodules with a design accelerating gradient of 5 MeV/m. Ongoing *in situ* processing has already resulted in an average gradient in excess of 7 MeV/m, which has made it possible to accelerate electrons to 5.5 GeV. The design maximum current is 200 μA CW, which can be split arbitrarily between three interleaved 499 MHz bunch trains. One such bunch train can be peeled off to any one of the Halls after each linac pass using RF separators and septa, while all Halls can simultaneously receive the maximum energy beam. Hall B with its large-acceptance detector CLAS requires a current as low as 1 nA, while a 100 μA beam is being delivered to one or even both of the other Halls. Hall C has been operational since November 1995, Hall A since May 1997 and Hall B since December 1997.

3 Nucleon Form Factors

Knowledge of the electromagnetic form factors (EMFF) is fundamental for the underlying structure of nucleons. The spatial distribution of the charge and

magnetization density within the nucleons provides sensitive tests of models based on QCD.

3.1 The Neutron Electric Form Factor

The neutron is an electrically neutral object that, in a naive quark model, is expected to be neutral even on a microscopical scale. Existing data indicate, however, that the neutron has a positively charged core surrounded by a negatively charged cloud. In a classical picture this is interpreted that the neutron spends part of the time as a proton and a negatively charged pion. Experimental studies of the neutron electric form factor have been hampered by the absence of a free neutron target. The recent availability of intense beams of highly polarized electrons and of dense highly polarized targets make it possible to accurately measure the neutron electric form factor through a variety of techniques which will for the first time allow a careful study of systematic errors in the data.

The $^2\vec{H}(\vec{e},e'n)$ reaction

Calculations of deuteron properties can be reliably performed in a variety of models. A polarized deuteron target can therefore to a very good approximation be used as an effective polarized neutron target[1]. A measurement of the asymmetry in the $^2\vec{H}(\vec{e},e'n)$ reaction[2] is being performed in Hall C to determine the product of G_E^n and G_M^n. In addition, a comparison with the measured asymmetry in the $^2\vec{H}(\vec{e},e'p)$ reaction will provide an experimental check on reaction mechanism predictions.

A polarized ammonia target, using the dynamic nuclear polarization (DNP) technique, originally designed for measurements of nucleon spin structure functions at SLAC, was adapted to the Hall C intrumentation. The target (see fig. 2) consists of a superconducting dipole, operating at 5 T, and a ^4He evaporation refrigerator, operating at 1 K. The target material, either NH_3 or ND_3, is doped by irradiation with paramagnetic centers (unpaired electrons), which will be nearly 100 % polarized at 5 T and 1 K. Ammonia with ^{15}N is used so that any polarization of the nitrogen is carried by just the odd proton and not also by a neutron as in ^{14}N. The electron polarization is transferred to the protons or deuterons by irradiation with microwaves (140 GHz at 5 T). This DNP technique has resulted in a polarization degree of close to 100(50) % for protons(deuterons). Radiation damage of the target material by the beam will cause the polarization to drop, but this can be largely recovered by annealing, i.e. warming the target to appr. 100 K. The beam is rastered over the full target area to minimize the local radiation dose.

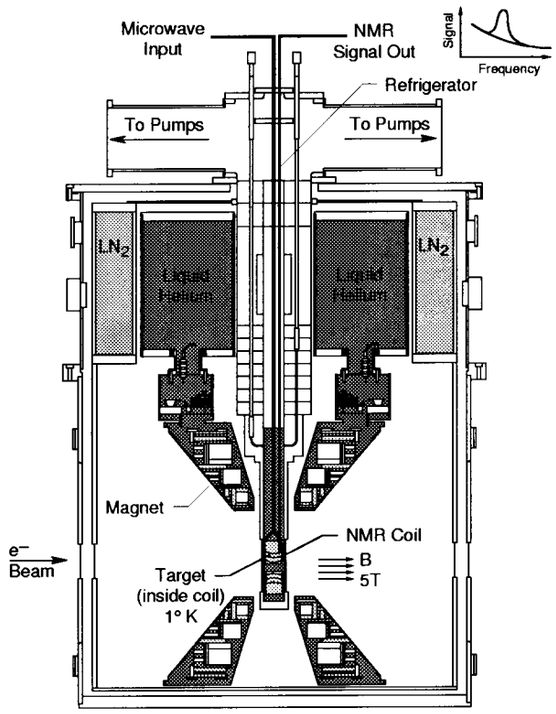

Figure 2: Lay-out of the polarized ammonia DNP target.

Scattered electrons are detected in the HMS spectrometer, while knocked-out neutrons (and protons) are detected in coincidence in a plastic scintillator array. The size of the neutron detector is fixed by the angular acceptance required to match that of the HMS at a distance large enough to provide an accurate time-of-flight measurement. The final design was a detector of 2.6 x 1.3 m^2, placed at a distance ranging from 3.4 to 8 m from the target for Q^2-values of 0.5 to 2.0 $(GeV/c)^2$. The total scintillator thickness of 30 cm results in a direct neutron detection efficiency of about 40 %. In the front of the detector a thin layer of scintillators provides particle identification and lead shielding is used as required to limit the background conditions to acceptable values.

To extract an asymmetry proportional to G_E^n, the target holding field has to be oriented in the scattering plane, perpendicular to $\vec{q}$. A magnetic chicane deflects the beam upstream of the target to be horizontal at the target position and downstream to center on the beam dump. The beam polarization is measured with a Møller polarimeter in which the target is magnetized to saturation perpendicular to its plane, using a 4 T superconducting split coil.

Measurements will be performed at three Q^2-values of 0.5, 1.0 and 1.7 $(GeV/c)^2$ with a projected uncertainty in G_E^n ranging from 9 % at 0.5 $(GeV/c)^2$ to 20 % at 1.7 $(GeV/c)^2$. Thus far, an average target polarization of close to 30 % has been observed on ND_3 with a beam of 125 nA and of over 70 % polarization.

The $^2H(\vec{e}, e'\vec{n})$ reaction

As a general equivalent to the use of a polarized target one can measure the polarization of the recoiling or knocked-out particle. Thus, the $^2H(\vec{e}, e'\vec{n})$ reaction also allows one to determine the neutron electric form factor G_E^n. Such an experiment[3] has been approved to run in Hall C.

A high-intensity highly polarized electron beam is scattered off a 12 cm long liquid deuterium target. The scattered electron is detected in the HMS spectrometer, and the knocked-out neutron is analyzed in a neutron polarimeter. The polarimeter utilizes the properties of n-p scattering as a polarization analyzer to measure the sideways polarization component of the neutron (perpendicular to $\vec{q}$). It consists of four liquid scintillators as an active analyzer and two sets of plastic scintillator rear detectors. The rear detectors are placed at azimuthal angles of 0^o and 180^o. The neutron energy is determined withm a resolution of appr. 5 % by measuring its flight time. The polarimeter will be encased in 240 cm thick concrete with a 10 cm thick lead collimator. By precessing the neutron spin with a dipole magnet until the transverse polar-

ization vanishes, one obtains a direct estimate of the ratio of G_E^n and G_M^n with minimal systematic uncertainties from beam polarization and polarimeter analyzing power. This experiment aims to measure G_E^n at three Q^2-values of 0.5, 1.0 and 1.7 $(\mathrm{GeV}/c)^2$ with a total error of 5-8 %.

The $^3\vec{H}e(\vec{e},e'n)$ reaction

The electric form factor of the neutron will also be measured[4] in Hall A using the $^3\vec{H}e(\vec{e},e'n)$ reaction in quasi-elastic kinematics, initially at a Q^2-value of 1 $(\mathrm{GeV}/c)^2$. Here, the ^3He nucleus serves as a polarized neutron, where the spins of the proton pair predominantly cancel each other. This reaction has become accessible, since dense polarized ^3He targets can be readily produced, either through the spin-exchange or the metastability-exchange technique.

The polarized target (see fig. 3) uses the principle of spin-exchange between optically-pumped rubidium vapor and ^3He nuclei. A central feature of the target is a glass cell, which contains ^3He at a pressure of nearly 10 atmosphere. The cell will have two connected chambers, an upper one in which the optical pumping and spin exchange takes place, and a lower one through which the electron beam passes. The upper chamber is heated to 170-200 ^{o}C to prevent condensation of the rubidium. The lower cell has a length of 40 cm, thus providing an integrated target density of 10^{22} atoms/cm^2.

The spin-exchange rate is governed to first approximation by the available laser power. Four diode arrays will provide about 80 W of usable laser light at a wavelength of 795 nm. The ^3He polarization decreases in time due to four independent effects: depolarization by the electron beam, relaxation by ^3He-^3He collisions and by ^3He collisions with the cell wall and by magnetic field inhomogeneities. A total depolarization rate of appr. 1/16 hours is expected at an electron current of 15 μA, resulting in an average target polarization of up to 50 %. Target polarimetry will be performed by two means. During the experiment the polarization will be monitored with the NMR technique of adiabatic fast passage. These signals will be calibrated by comparing the signals with those from water. This calibration will be verified by studying the frequency shift that the ^3He nuclei induce on the electromagnetic resonance lines of the Rb atoms.

The scattered electrons will be detected in one of the high-resolution spectrometers (HRS) and the kocked-out neutrons in a plastic scintillator array of 120 x 120 cm^2 and a total thickness of 30 cm in three layers of 10 cm each. The neutron detector will be placed in a shielding hut of 120 cm of high-density concrete, while a 10 cm lead window in front of the detector will degrade all gamma rays to below the detector thresholds. The overall detector efficiency

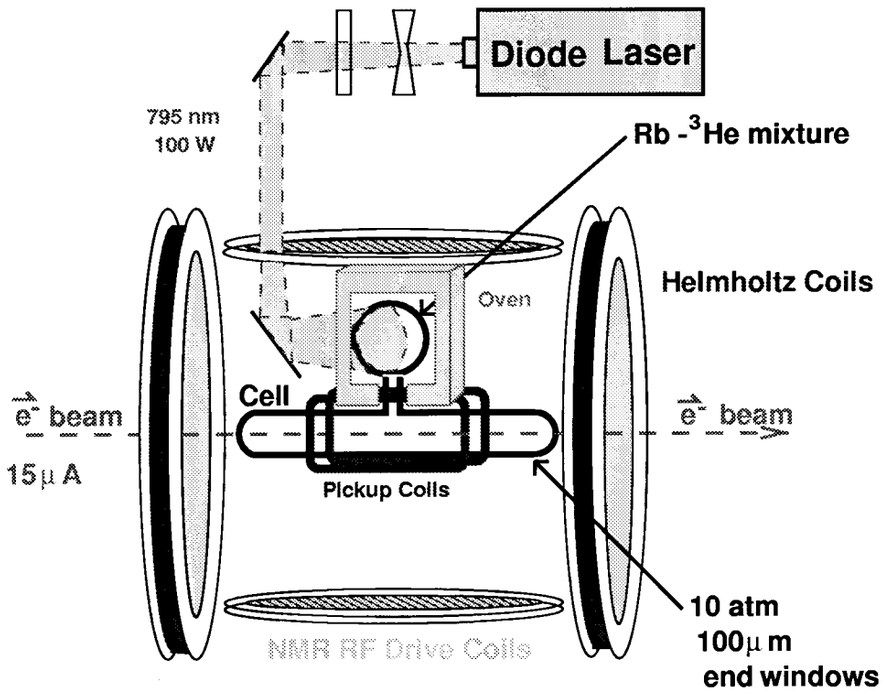

Figure 3: Schematic lay-out of the polarized ^3He target.

is expected to be about 12 % with an angular acceptance of 6 msr.

The beam asymmetry for the $^3\vec{H}e(\vec{e},e'n)$ reaction will be measured with the target spin oriented perpendicular and longitudinal to $\vec{q}$. The ratio of these asymmetries is directly proportional to G_E^n, without requiring an accurate knowledge of either the target or the beam polarization. The projected total error in the G_E^n measurement at 1 $(\mathrm{GeV}/c)^2$ is 8 %.

Summary

Figure 4 presents an overview of existing data of G_E^n and of results expected within the near future. The shaded band indicates the systematic error in the most recent unpolarized measurement[5] due to different assumptions for the N-N potential. The first results with a polarized target obtained about five years ago at Bates[6,7] already indicated the potential of the new technique. The recent results from Mainz obtained with high accuracy from both the $^2H(\vec{e},e'\vec{n})$ and $^3\vec{H}e(\vec{e},e'n)$ reaction have already inspired several detailed studies of reaction mechanism corrections in each of the nuclear systems. Clearly dedicated experimental studies are required to confirm such predictions, but the NIKHEF measurements at 0.22 $(\mathrm{GeV}/c)^2$ will already provide a sensitive test bench. With the JLab results, expected from all three reactions within the next few years, an accurate data set on G_E^n will be available for Q^2-values up to 2 $(\mathrm{GeV}/c)^2$.

3.2 The Proton Electric Form Factor

Elastic electron scattering off the proton has been measured[13] up to Q^2-values of 31 $(\mathrm{GeV}/c)^2$. However, already at fairly modest values of Q^2 the contribution from the magnetic form factor G_M^p is so dominant that a reliable Rosenbluth separation becomes extremely difficult. This is already evident (see fig. 5) from the large scatter in the existing data set on G_E^p. The electric form factor of the proton has been calculated within the framework of either the vector meson dominance (VMD) model or QCD-based quark models. In general VMD calculations predict G_E^p to decrease faster than G_{dipole} with increasing Q^2. It is certainly not yet obvious whether the quark structure of the hadrons plays a detectable role at intermediate Q^2-values.

Recently an experiment[14] of G_E^p has been completed in Hall A in which longitudinally polarized electrons were scattered off a liquid hydrogen target. The polarization of the recoiling proton was measured with a Focal Plane Polarimeter (FPP), in coincidence withe the scattered electron. In this technique the electric form factor G_E^p is measured directly through an interference term with G_M^p, thus offering a significant improvement on the systematic error. The

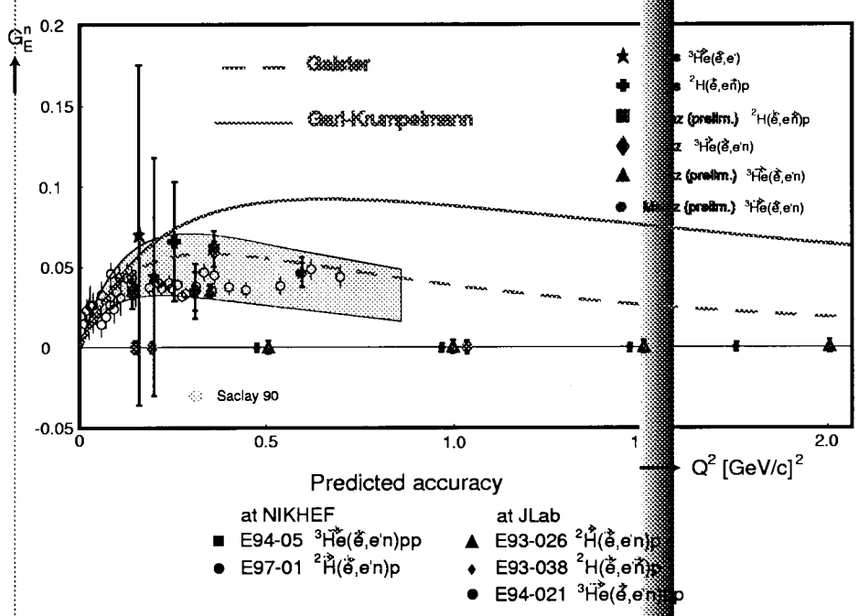

Figure 4: World data set for G_E^n as a function of Q^2: open circles[5], stars[6], cross[7], squares[8], diamond[9], triangle[8] and circle[10]. Theory: solid[11], dashed[12].

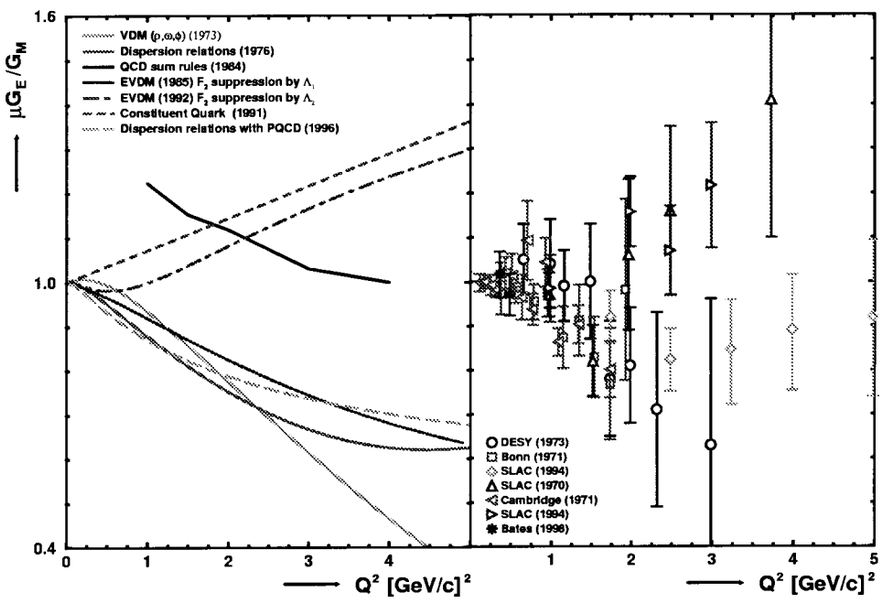

Figure 5: Theoretical predictions(left) and world data set(right) for the ratio of G_E^p and G_M^p as a function of Q^2: squares[15], left triangles[16], circles[17], diamonds[18], right triangles[19].

FPP, installed in the focal plane of the hadron HRS, consists of a carbon analyzer sandwiched between two pairs of straw tube drift chambers. A variety of carbon slabs, with a total thickness of up to 60 cm, can be selected remotely in order to optimize the figure of merit at each Q^2-setting. The helicity of the electron beam was changed every 15 ms pairwise-randomly and the ratio of the longitudinal to the transverse polarization of the recoiling proton was measured. This ratio is directly proportional to that between G_E^p and G_M^p and knowledge of either the beam polarization or the FPP analyzing power is not required.

Data were taken at four Q^2-settings between 1.7 and 3.5 $(\mathrm{GeV}/c)^2$ with a thin wafer of bulk GaAs in the polarized source, which provided a beam in Hall A with a polarization of 40 % and an average intensity of close to 100 μA over a month of running. In a second run four additional measurements were performed covering a Q^2-range of 0.5 to 1.5 $(\mathrm{GeV}/c)^2$, but now with a strained GaAs wafer, providing a beam polarization of 65 % at an intensity

larger than 10 μA. A preliminary analysis yielded a value for G_E^p of about half the G_{dipole}-value at 3.5 (GeV/c)^2. The final results are expected to have a total precision of about 7 %.

3.3 The Neutron Magnetic Form Factor

Recently the results of a several new measurements [20,21] of the neutron magnetic form factor G_M^n using deuteron targets have become available at low Q^2-values. Although these new data sets each have been assigned significantly reduced statistical and systematic uncertainties, large discrepancies exist between the various data sets (see fig. 6). A precise knowledge of G_M^n is very important also for the extraction of the strange electric and magnetic form factors of the nucleon from the results of parity-violation measurements.

Recently, Ishikawa et al.[22] have included the effects of final-state interactions (FSI) in calculations of the transverse asymmetry in inclusive quasi-elastic scattering from ^3He. The systematic uncertainty in extracting the neutron magnetic form factor from $A_{T'}$ was determined to be less than 2 %. In the approved proposed experiment[23] $A_{T'}$ will be measured in a 20 MeV wide bin on top of the quasi-elastic peak with a 2 % statistical uncertainty at five Q^2-values between 0.1 and 0.5 (GeV/c)^2. The same target set-up will be used as in the G_E^n measurement with the $^3\vec{H}e(\vec{e},e'n)$ reaction, described earlier. The product of beam and target polarization will be monitored during the experiment by a simultaneous measurement of the elastic asymmetry in the second HRS spectrometer.

4 The Deuteron

As the only bound two-baryon system, the deuteron plays a crucial role in the study of the strong nucleon-nucleon interaction. In particular the deuteron EMFF's offer unique opportunities to test various models of the short-range and the tensor components of the N-N interaction, of meson-exchange currents and isobaric configurations, as well as to investigate the possible role of explicit quark degrees of freedom.

4.1 Deuteron Form Factors A and B

Because of the spin-one ground state of the deuteron, elastic scattering off it is characterized by three form factors: the charge monopole G_C, the charge quadrupole G_Q and the magnetic dipole G_M. The standard Rosenbluth separation technique allows the determination of two structure functions A and B, where B is directly proportional to G_M and A is a linear combination of G_C, G_Q

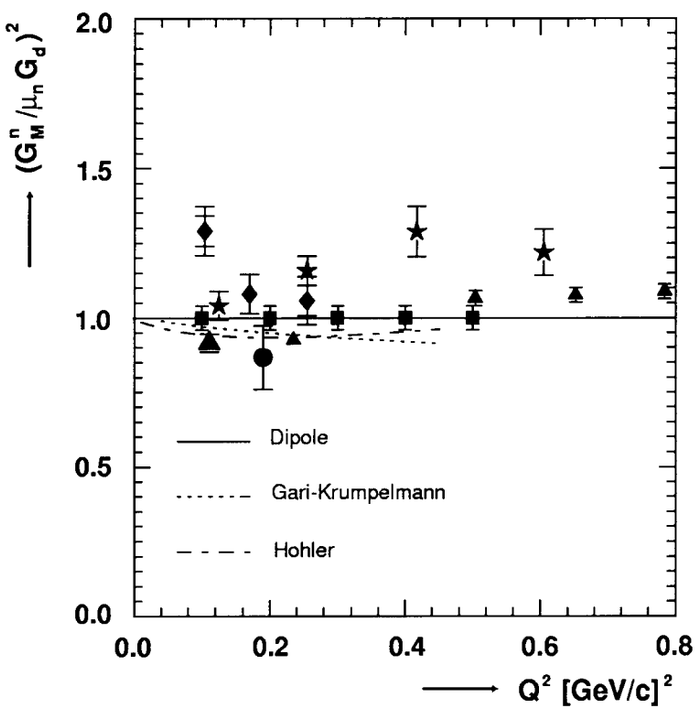

Figure 6: Existing and projected (solid squares) data for the ratio of G_M^n and G_{dipole} as a function of Q^2: triangles[20], stars[21], diamonds[24] and circle[25]. Theory: full (dipole parametrization G_{dipole}), dotted[11], dashed[26].

and G_M. The existing world data set on A(Q^2) is limited to Q^2 of 4 (GeV/c)^2 and significant discrepancies exist between data around 1 (GeV/c)^2.

In a recent experiment[27] in Hall A the elastic electron-deuteron cross section was measured in a Q^2-range from 0.7 to 6.0 (GeV/c)^2. To suppress background and to separate elastic from inelastic processes, recoil deuterons were detected in the HRSH spectrometer in coincidence with the scattered electrons in the HRSE spectrometer. Electron beams of up to 100 μA were scattered off a 15 cm long liquid deuterium target, resulting in a luminosity of 4.0 x 10^{38} atoms/cm^2/s. At the highest Q^2-value of 6 (GeV/c)^2 the elastic cross section was measured to be 2 x 10^{-41} cm^2/sr, at two counts per day. Values for A(Q^2) were extracted from the data under the assumption that the contribution from B(Q^2) can be neglected. The systematic error was estimated to be 8 %, while the statistical error ranged from 1 to 30 %. The data exhibit a smooth fall-off with Q^2 and confirm the trend of the SLAC[28] data, in contrast to that of the Bonn[15] and CEA[16] data.

The data (see fig. 7) are compared to the results[29,30] of two relativistic calculations. Although the data clearly favour the model of Van Orden et al., a definitive test of such relativistic calculations (including MEC effects) should include all three deuteron form factors. The results for B(Q^2) in a Q^2-range from 0.7 to 1.4 (GeV/c)^2 are expected to be available within a couple of months.

4.2 Tensor Analyzing Power

In order to separate all three EMFF's for the deuteron at least one measurement has to be performed with either a polarized target or a recoil polarimeter. The tensor analyzing power T_{20} measured in those experiments contains an interference term between G_C and G_Q. T_{20} is directly sensitive to the tensor component in the N-N interaction (it would be zero in the absence of it). A large variety of theoretical studies have been focussed on T_{20}, which can be classified in a general sense, according to the use of a relativistic framework[29,30] or of a nucleon potential model[31,32]. The agreement between different experimental techniques can not be tested directly, since the data do not cover overlapping Q^2-ranges (from 0.08 to 0.36 (GeV/c)^2 for experiments with polarized internal targets[33] and from 0.58 to 0.85 (GeV/c)^2 for those using a recoil polarimeter[34]) (see fig. 8). It is interesting to note, however, that the former favor nucleon potential model calculations (including MEC effects) while the latter are well described by relativistic calculations. The then available data on T_{20} led Henning et al.[35] to point out an inconsistency in the location of the minimum of the charge form factor in two- and three-nucleon systems.

In a recent experiment[36] in Hall C T_{20} was measured in a Q^2-range from

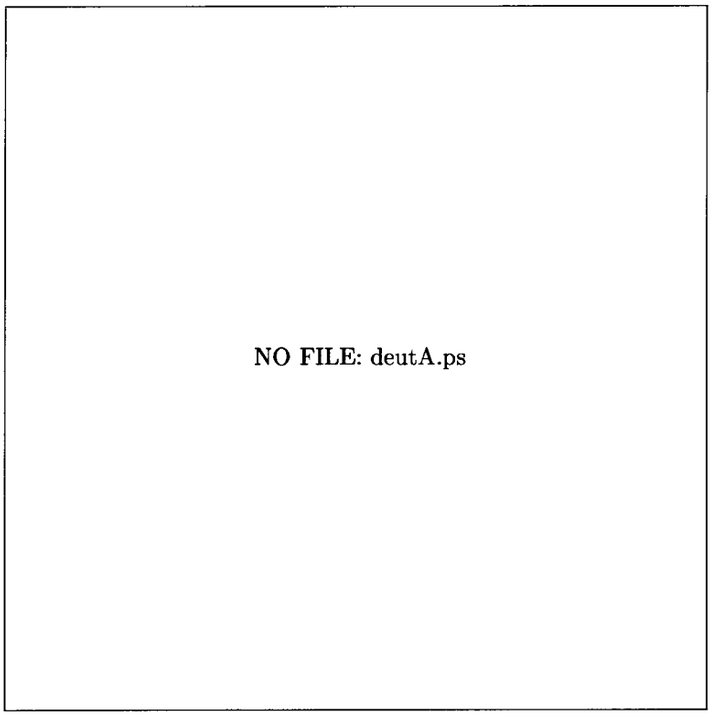

Figure 7: Data for A(Q^2) from the JLab experiment compared to RIA calculations[29,30]. Earlier SLAC data[28] are also shown.

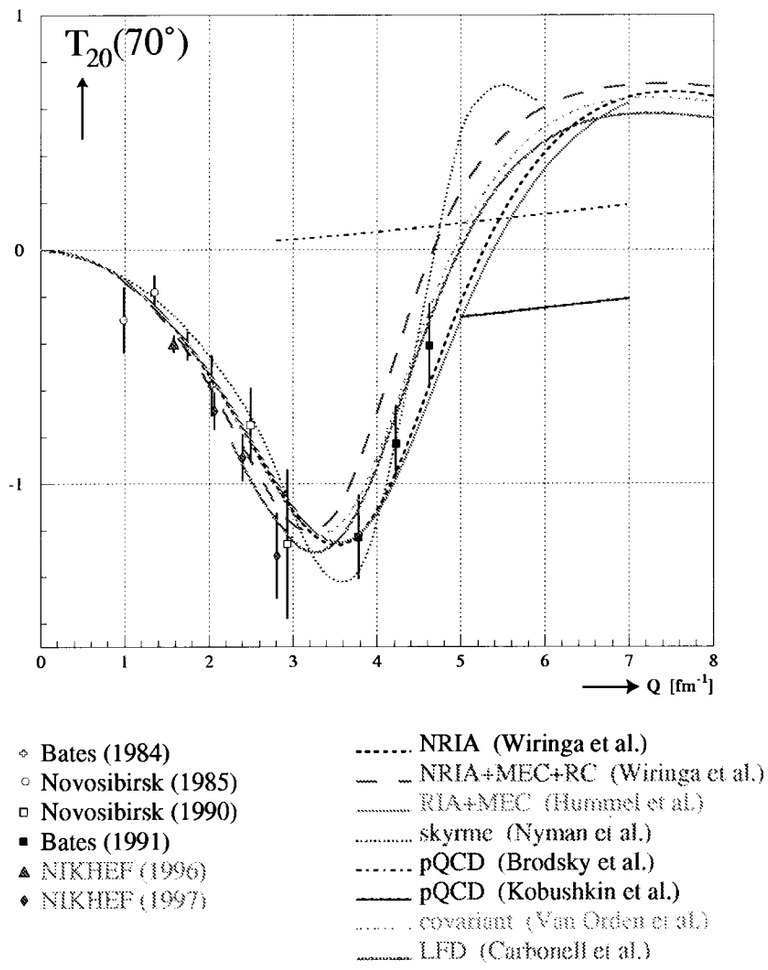

Figure 8: World data set (see ref.[33] for details) for T_{20} as a function of Q^2.

4.0 to 6.8 fm^{-1}. An electron beam of 100 μA was scattered off a 12 cm long liquid deuterium target. The scattered electrons were detected in the HMS spectrometer, the recoiling deuterons were analyzed in a dedicated polarimeter(POLDER). POLDER utilizes the $^1H(\vec{d},2p)n$ reaction, which provides a high figure of merit for deuteron energies up to 500 MeV. The purpose of the first part of the deuteron arm is to focus the maximum number of deuterons on the polarimeter target, while shielding it from a direct line of sight from the electron target. Proper deuteron identification is provided by time-of-flight and energy deposit measurements in two fast plastic scintillators. The $^1H(\vec{d},2p)n$ reaction takes place in a 16 cm long LD_2 target. The protons created in the $^1H(\vec{d},2p)n$ reaction are detected in two scintillator hodoscopes. The polarimeter was calibrated at Saturne for incident deuteron energies ranging between 175 and 500 MeV. Since POLDER samples the full angular dependence, data will also be obtained for T_{21} and T_{22}.

4.3 The Break-up Channel

The tensor component of the N-N interaction is responsible for the D-state component in the predominantly S-wave ground-state wave function of the deuteron and causes its density distribution to depend on the spin projection. In combination with the short-range repulsive core this causes the deuteron to exhibit a toroidal shape for m_z= 0 and a dumbbell shape for m_z= 1 (see fig. 9). This spin-dependent density distribution can be probed by studying the break-up channel from tensor-polarized deuterons, whereas elastic scattering probes the total nuclear current distribution. First results for such an experiment have been reported[38], performed at the internal target facility at NIKHEF, but the range in missing-momentum p_m covered was limited to approximately 150 MeV/c.

With a DNP ND_3 target as described earlier, also tensor polarization can be obtained by inducing specifically the hyperfine transitions to the m_z= 0 state. A proposal[39] has been approved to measure the tensor analyzing power in the break-up reaction on the deuteron, using basically the same instrumentation in Hall C as for the G_E^n-experiment. The polarization axis now has to be oriented parallel to Q^2, implying that the chicane has to produce a downward incoming beam. The knocked-out protons will be detected in the SOS spectrometer. The tensor analyzing power will be measured over a p_m-range from 200 to 375 MeV/c with a total error of 10-15 %. This range fully covers the minimum predicted at around 300 MeV/c in the spin-dependent cross section for the m_z= 1 state.

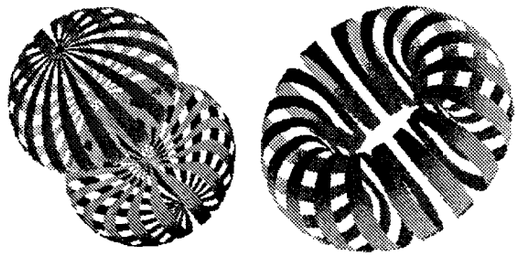

Figure 9: The equidensity surfaces of the deuteron density distribution for $m_z = 1$ (left) and $m_z = 0$ (right) from Forest et al.[37].

5 Summary

An overview has been presented of the research program at Jefferson Lab focused on nucleonic properties and few-body systems. First results presented in this paper indicate the high quality which can be expected in the next few years, in a significant part due to the truely impressive properties of the beam at JLab.

Acknowledgments

The author would like to thank the spokespersons of the experiments described in this report for providing detailed information and, where possible, preliminary results of their experiments. This work was supported in part by the U.S. Department of Energy and National Science Foundation.

References

1. R. Arnold, C. Carlson, and F. Gross, *Phys. Rev.* C **23**, 363 (1981).
2. D. Day and J. Mitchell, JLab proposal E93-026.
3. R. Madey and S. Kowalski, JLab proposal E93-038.
4. W. Korsch and R. McKeown, JLab proposal E94-021.
5. S. Platchkov et al., *Nucl. Phys.* A **510**, 740 (1990).
6. A.K. Thompson et al., *Phys. Rev. Lett.* **68**, 2901 (1992).
7. T. Eden et al., *Phys. Rev.* C **50**, R1749 (1994).
8. F. Klein, Proc. of the 14th Int. Conf. on Particles and Nuclei, Williamsburg, 1996, p.121.
9. M. Meyerhoff et al., *Phys. Lett.* B **327**, 201 (1994).
10. D. Rohe, Ph.D. thesis, University of Mianz (1998).

11. M. Gari and W. Krumpelmann, *Z. Phys.* A **322**, 689 (1985).
12. S. Galster et al., *Nucl. Phys.* B **32**, 221 (1971).
13. R. Arnold et al., *Phys. Rev. Lett.* **57**, 174 (1986).
14. C. Perdrisat and V. Punjabi, JLab proposal E93-027.
15. R. Cramer et al., *Z. Phys.* C **29**, 513 (1985).
16. J.E. Elias et al., *Phys. Rev.* **177**, 2075 (1969).
17. W. Bartel et al., *Nucl. Phys.* B **58**, 429 (1973).
18. P. Bosted et al., *Phys. Rev. Lett.* **68**, 3841 (1992).
19. R.C. Walker et al., *Phys. Lett.* B **224**, 353 (1989).
20. H. Anklin et al., *Phys. Lett.* B **428**, 248 (1998).
21. E.E.W. Bruins et al., *Phys. Rev. Lett.* **75**, 21 (1995).
22. S. Ishikawa et al., *Phys. Rev.* C **57**, 39 (1998).
23. H. Gao, JLab proposal E95-001.
24. P. Markowitz et al., *Phys. Rev.* C **48**, R5 (1993).
25. H. Gao et al., *Phys. Rev.* C **50**, R546 (1994).
26. G. Höhler et al., NPB **114**, 505 (1976).
27. G. Petratos and J. Gomez, JLab proposal E91-026.
28. R. Arnold et al., *Phys. Rev. Lett.* **35**, 776 (1975).
29. E. Hummel and J.A. Tjon, *Phys. Rev.* C **42**, 423 (1990).
30. J.W. Van Orden, N. Devine and F. Gross, *Phys. Rev. Lett.* **75**, 4369 (1995).
31. B. Wiringa, V.G.J. Stoks and R. Schiavilla, *Phys. Rev.* C **51**, 38 (1995).
32. B. Mosconi, J. Pauschenwein and P. Ricci, *Phys. Rev.* C **48**, 332 (1993).
33. M. Bouwhuis et al., submitted to *Phys. Rev. Lett.*.
34. M. Garcon et al., *Phys. Rev.* C **49**, 2516 (1994).
35. H. Henning et al., *Phys. Rev.* C **52**, R471 (1995).
36. S. Kox and E. Beise, JLab proposal E94-018.
37. J.L. Forest et al., *Phys. Rev.* C **54**, 646 (1996).
38. Z.-L. Zhou et al., submitted to *Phys. Rev. Lett.*.
39. H. Anklin and W.U. Böglin, JLab proposal E97-102.